Estimation of Vehicle Roll and Road Bank Angle

Jihan Ryu
Design Division
Dept. of Mechanical Engineering
Stanford University
Stanford, CA 94305-4021
jihan@stanford.edu

J. Christian Gerdes
Design Division
Dept. of Mechanical Engineering
Stanford University
Stanford, CA 94305-4021
gerdes@stanford.edu

Abstract— **This paper presents a new method for identifying road bank and vehicle roll separately using a disturbance observer and a vehicle dynamic model. The authors have previously shown that vehicle states and parameters of a vehicle model can be precisely estimated using measurements from Global Positioning System (GPS) and Inertial Navigation System (INS) sensors. Based on these results, a dynamic model, which includes vehicle roll as a state and road bank as a disturbance, is first introduced. A disturbance observer is then implemented from the vehicle model using estimated vehicle states. Experimental results verify that the estimation scheme is giving appropriate estimates of the vehicle roll and road bank angles separately.**

I. INTRODUCTION

Vehicle stability control systems and state estimators commonly use lateral acceleration measurements from accelerometers to calculate lateral acceleration and sideslip angle of the vehicle [1], [2]. These acceleration measurements, however, are easily affected by disturbances such as road bank angle and vehicle roll induced by suspension deflection. Since these unwanted effects in acceleration measurements can lead to false estimation of the vehicle states or misleading activation of the stability control systems, knowledge of the vehicle roll and road bank angles is extremely important for such systems.

As a result, many researchers have pointed out that detection of the road bank angle and vehicle roll is necessary for the satisfactory performance of such systems [1], [2], [3]. Over the last few years, several methods were proposed to estimate the road bank angle, but the vehicle roll induced by suspension deflection was neglected or was lumped with the road bank angle [1], [2], [3], [4], [5], [6]. While a lumped value can be used to compensate the acceleration measurements, the separation of these two angles could be especially beneficial to vehicle rollover warning and avoidance systems [7], [8]. Since a small lumped value does not necessarily mean a small road bank angle, a vehicle may experience a significant road bank angle even though the sum of the two angles is small. The vehicle rollover warning or avoidance systems may need to be aware of this because a significant road bank angle can create different behavior of the vehicle during transient maneuvering, when most rollover accidents actually happen.

The main challenge in separating road bank angle and vehicle roll angle is that it is difficult to differentiate one from the other by using typical roll-related measurements (lateral acceleration and roll rate). Since the lateral accelerometers are usually attached to the vehicle body, the road bank angle and vehicle roll have the exact same effect on the lateral acceleration measurements and are not differentiable. The roll rate gyros are also attached to the vehicle body and can only see changes of the road bank and vehicle roll angles together, not individual changes separately. Therefore, vehicle roll and road bank angles cannot be directly separated using the kinematic relationships of the roll-related measurements.

Even though the vehicle roll and road bank angles have similar and indistinguishable influences on the measurements, they play very different roles in the vehicle dynamics. While the road bank angle can be treated as a disturbance or unknown input to the vehicle, the vehicle roll angle is a state resulting from the road bank angle and other inputs, governed by vehicle dynamics. This implies that a parameterized vehicle dynamic model could conceivably be used to separate the vehicle roll and road bank angles. The authors have previously shown that parameters of such a model can be precisely estimated using measurements from Global Positioning System (GPS) and Inertial Navigation System (INS) sensors [6]. It has been also shown that the sideslip angle and the sum of the vehicle roll and road bank angles can be accurately estimated from these sensors using only kinematic relationships.

Based on these results, this paper presents a new method for identifying road bank and vehicle roll separately using a disturbance observer and a vehicle dynamic model. First, a dynamic model, which includes vehicle roll as a state and road bank as a disturbance, is introduced. The disturbance observer is then implemented using the measurements of the sideslip angle, yaw rate, roll rate, and vehicle tilt angle (the sum of road bank and vehicle roll angles). The yaw rate and roll rate of the vehicle can be easily measured using rate gyros. The sideslip angle and vehicle tilt angle can be accurately determined using GPS and INS as demonstrated in previous work [6]. From the disturbance observer, road bank angle and vehicle roll can be separately estimated.

II. ROAD AND VEHICLE KINEMATICS

Fig. 1 shows a schematic diagram for a vehicle roll model with road bank angle. It is assumed that the vehicle body rotates around the roll center of the vehicle. In Fig. 1, h is the height of the center of gravity (CG) from the roll center.

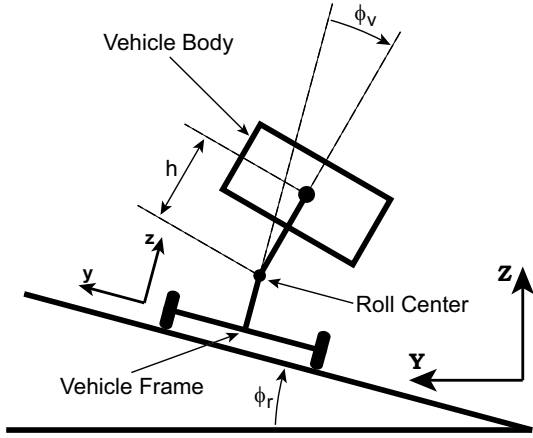ϕ_v and ϕ_r are the vehicle roll angle and road bank angle respectively.

Fig. 1.   Vehicle Roll Model

If a roll rate gyro is attached to the vehicle body in Fig. 1, one might assume the roll rate gyro measures $\dot{\phi}_v + \dot{\phi}_r$, the sum of the rate of change of vehicle roll angle and the rate of change of road bank angle. However, this is not what the roll rate gyro really measures. To illustrate this, assume a vehicle follows a circular path on a large flat plane with a slope of 10 degrees from the horizontal, and the vehicle has no roll from suspension deflection ($\phi_v = 0$). The vehicle will then experience a road bank angle, ϕ_r, that changes from -10 to 10 degrees in one revolution of the circle. In this case, $\dot{\phi}_r$ is definitely not zero since the road bank angle experienced by the vehicle, ϕ_r, is continuously changing. However, the roll rate measurement is always zero because the angular velocity vector of the vehicle is orthogonal to the axis of the roll rate gyro and as a result the roll rate gyro cannot sense the change of the road bank angle. As this example shows, a careful treatment of the kinematics is necessary before a disturbance observer for estimating the vehicle and road bank angles can be implemented.

In this paper, the vehicle frame is assumed to keep contact with the ground. Under this assumption, the roll and pitch motions of the vehicle frame are totally constrained by the road, and the road bank angle and road grade are the same as the roll and pitch angles of the vehicle frame in the inertial frame. Consequently, the attitude of the vehicle frame with respect to the inertial coordinates is first defined by the Euler angles in this paper, and the rate of change of the road bank angle is expressed in terms of the angular velocities of the vehicle frame.

When the rotation of the vehicle frame is given by the Euler angles (ψ, θ, ϕ) about vehicle-frame-fixed axes according to the ISO standard, where the first rotation is by an angle ψ about the z axis, the second is by an angle θ about the y axis, and the third is by an angle ϕ about the x axis, the transformation matrix from the inertial coordinates to the vehicle-frame-fixed coordinates is given in Eq. (1):

$$
\begin{aligned}
Q_{30} &= Q_{32}Q_{21}Q_{10} \\
Q_{32} &= \begin{bmatrix} 1 & 0 & 0 \\ 0 & \cos\phi & \sin\phi \\ 0 & -\sin\phi & \cos\phi \end{bmatrix} \\
Q_{21} &= \begin{bmatrix} \cos\theta & 0 & -\sin\theta \\ 0 & 1 & 0 \\ \sin\theta & 0 & \cos\theta \end{bmatrix} \\
Q_{10} &= \begin{bmatrix} \cos\psi & \sin\psi & 0 \\ -\sin\psi & \cos\psi & 0 \\ 0 & 0 & 1 \end{bmatrix}
\end{aligned} \tag{1}
$$

The subscript 0 indicates the inertial coordinates and the subscript 3 represents the vehicle-frame-fixed coordinates. Similarly, the subscript 1 describes the intermediate coordinates given by the rotation about the z axis from the inertial coordinates 0, and the subscript 2 denotes the intermediate coordinates given by the rotation about the y axis from the intermediate coordinates 1.

The angular velocity vector of the vehicle frame with respect to the inertial coordinates, which is expressed in the vehicle-frame-fixed coordinates, is defined as:

$$
\omega_{30,3} = \begin{bmatrix} p_f & q_f & r_f \end{bmatrix}^T \tag{2}
$$

where p_f, q_f, and r_f represent the x, y, and z components of the angular velocity vector, $\omega_{30,3}$. The first two subscripts 30 mean that $\omega_{30,3}$ is the angular velocity of 3 (the vehicle frame) with respect to 0 (the inertial frame), and the last subscript 3 means the vector is expressed in 3 (the vehicle-frame-fixed coordinates).

Using Eq. (1), the relationship between the vehicle-frame-fixed angular velocity vector, $\omega_{30,3}$, and the rate of change of the Euler angles, $\begin{bmatrix} \dot{\psi} & \dot{\theta} & \dot{\phi} \end{bmatrix}^T$, can be determined by resolving the Euler rates into the vehicle-frame-fixed coordinates:

$$
\begin{aligned}
\begin{bmatrix} p_f \\ q_f \\ r_f \end{bmatrix} &= Q_{32}\begin{bmatrix} \dot{\phi} \\ 0 \\ 0 \end{bmatrix} + Q_{32}Q_{21}\begin{bmatrix} 0 \\ \dot{\theta} \\ 0 \end{bmatrix} + Q_{32}Q_{21}Q_{10}\begin{bmatrix} 0 \\ 0 \\ \dot{\psi} \end{bmatrix} \\
&= J\begin{bmatrix} \dot{\phi} \\ \dot{\theta} \\ \dot{\psi} \end{bmatrix}
\end{aligned} \tag{3}
$$

The Euler rates can be then determined from the vehicle-frame-fixed angular velocity vector by inverting J:

$$
\begin{bmatrix} \dot{\phi} \\ \dot{\theta} \\ \dot{\psi} \end{bmatrix} = \begin{bmatrix} 1 & \sin\phi\tan\theta & \cos\phi\tan\theta \\ 0 & \cos\phi & -\sin\phi \\ 0 & \sin\phi/\sin\theta & \cos\phi/\cos\theta \end{bmatrix}\begin{bmatrix} p_f \\ q_f \\ r_f \end{bmatrix} \tag{4}
$$

$$
\therefore \dot{\phi} = p_f + \sin\phi\tan\theta\, q_f + \cos\phi\tan\theta\, r_f \tag{5}
$$

When the Euler angle θ is not zero, the Euler angle ϕ is not the same as the road bank angle, ϕ_r, illustrated in Fig. (1), because the road bank angle is defined between the vehicle frame and the intermediate coordinates 1. Similarly, $\dot{\phi}_r$ is not the same as $\dot{\phi}$ unless θ is zero.

However, $\dot{\phi}_r$ is the x component of the angular velocity, $\omega_{31,1}$, since $\omega_{31,1}$ represents the angular velocity of the vehicle frame with respect to the intermediate coordinates $_1$. Therefore, the rate of change of the road bank angle, $\dot{\phi}_r$, is given by the following equation:

$$\omega_{31,1} = \begin{bmatrix} \dot{\phi}_r \\ \dot{\theta}_r \\ \dot{\psi}_r \end{bmatrix} = Q_{12} \begin{bmatrix} \dot{\phi} \\ 0 \\ 0 \end{bmatrix} + \begin{bmatrix} 0 \\ \dot{\theta} \\ 0 \end{bmatrix} \tag{6}$$

$$= Q_{21}^{-1} \begin{bmatrix} \dot{\phi} \\ 0 \\ 0 \end{bmatrix} + \begin{bmatrix} 0 \\ \dot{\theta} \\ 0 \end{bmatrix} = \begin{bmatrix} \cos\theta\,\dot{\phi} \\ \dot{\theta} \\ -\sin\theta\,\dot{\phi} \end{bmatrix} \tag{7}$$

$$\therefore \dot{\phi}_r = \cos\theta\,\dot{\phi} \tag{8}$$

where ϕ_r and θ_r represent the road bank angle and road grade respectively. Using Eq. (5), Eq. (8) can be rewritten as:

$$\dot{\phi}_r = \cos\theta\,p_f + \sin\phi\sin\theta\,q_f + \cos\phi\sin\theta\,r_f \tag{9}$$

Since the yaw rate gyro and the roll rate gyro are attached to the vehicle body, the yaw and roll rates of the vehicle frame, r_f and p_f respectively, cannot be exactly measured. The yaw rate and roll rate measurements include the effects of vehicle roll motion. Since the vehicle-body-fixed coordinates are defined from a rotation by the angle ϕ_v about the x axis of the vehicle-frame-fixed coordinates, the transformation matrix from the vehicle-frame-fixed coordinates to the vehicle-body-fixed coordinates is given by:

$$Q_{43} = \begin{bmatrix} 1 & 0 & 0 \\ 0 & \cos\phi_v & \sin\phi_v \\ 0 & -\sin\phi_v & \cos\phi_v \end{bmatrix} \tag{10}$$

where the subscript $_4$ indicates the vehicle-body-fixed coordinates.

Using Eq. (10), The yaw rate measurement, r_m, and the roll rate measurement, p_m, can written as:

$$\omega_{40,4} = \begin{bmatrix} p_m \\ q_m \\ r_m \end{bmatrix} = \begin{bmatrix} \dot{\phi}_v \\ 0 \\ 0 \end{bmatrix} + Q_{43} \begin{bmatrix} p_f \\ q_f \\ r_f \end{bmatrix} \tag{11}$$

$$p_m = p_f + \dot{\phi}_v \tag{12}$$

$$\therefore r_m = \cos\phi_v\,r_f - \sin\phi_v\,q_f \tag{13}$$

where p_m and r_m are from rate gyros attached to the vehicle body. Note that Eq. (12) says that the roll rate measurement, p_m, is not the same as $\dot{\phi}_v + \dot{\phi}_r$, the sum of the rate of the vehicle roll angle change and the rate of the road bank angle change as explained in the beginning of this section.

Eq. (9) can be rewritten by defining a new variable ε_r and assuming the vehicle pitch angle θ is small and so $\cos\theta$ is close to one:

$$\dot{\phi}_r \approx p_f + \varepsilon_r \tag{14}$$

where

$$\varepsilon_r = \sin\phi\sin\theta\,q_f + \cos\phi\sin\theta\,r_f$$

Eq. (13) can be also simplified as Eq. (15) assuming the vehicle roll angle, ϕ_v, and the pitch rate, q_f, are small:

$$r_m \approx r_f \tag{15}$$

III. Vehicle Model

The dynamics of a vehicle are represented here by the single track, or bicycle model with a roll mode [8]. It is assumed that the slip angles on the inside and outside wheels are approximately the same. Fig. 2 shows a schematic diagram for the vehicle model. In Fig. 2, δ represents the
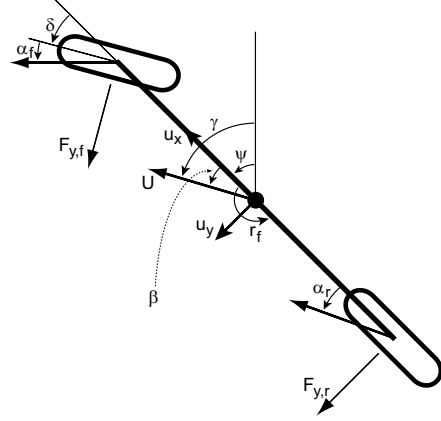

Fig. 2.   Single Track Model

steering angle. u_x and u_y are the longitudinal and lateral components of the vehicle velocity at the center of the vehicle frame in the vehicle frame fixed coordinates, and r_f is the yaw rate of the vehicle frame. β is the sideslip angle at the center of the vehicle frame. F_{yf} and F_{yr} are the lateral tire forces, and α_f and α_r are the tire slip angles.

Linearized with the small angles and a linear tire model, F_{yf} and F_{yr} become:

$$F_{yf} = -C_{\alpha f}\alpha_f, \quad F_{yr} = -C_{\alpha r}\alpha_r \tag{16}$$

The equations of motion can be then linearized as in Eq. (17), (18), and (19) assuming the road changes smoothly:

$$\dot{\beta} = -\frac{I_{eq}C_0}{I_x m u_x}\beta - \left(1 + \frac{I_{eq}C_1}{I_x m u_x^2}\right)r_f + \frac{h(mgh - k_r)}{I_x u_x}\phi_v$$
$$- \frac{hb}{I_x u_x}\dot{\phi}_v + \frac{I_{eq}C_{\alpha f}}{I_x m u_x}\delta - \frac{g}{u_x}\phi_r \tag{17}$$

$$\dot{r}_f = -\frac{C_1}{I_z}\beta - \frac{C_2}{I_z u_x}r_f + \frac{aC_{\alpha f}}{I_z}\delta \tag{18}$$

$$\ddot{\phi}_v = -\frac{C_0 h}{I_x}\beta - \frac{C_1 h}{I_x u_x}r_f + \frac{mgh - k_r}{I_x}\phi_v - \frac{b_r}{I_x}\dot{\phi}_r$$
$$+ \frac{C_{\alpha f}h}{I_x}\delta - \dot{p}_f \tag{19}$$

where

$$C_0 = C_{\alpha f} + C_{\alpha r}, \quad C_1 = aC_{\alpha f} - bC_{\alpha r}$$
$$C_2 = a^2 C_{\alpha f} + b^2 C_{\alpha r}, \quad I_{eq} = I_x + mh^2$$

I_z is the moment of inertia of the vehicle about its yaw axis and m is the mass of the vehicle, which is assumed

to have no vehicle frame mass. a and b are distance of the front and rear axles from the CG, and $C_{\alpha f}$ and $C_{\alpha r}$ are the total front and rear cornering stiffness. I_x is the moment of inertia about the roll axis, k_r is the roll stiffness, and b_r is the roll damping coefficient. h is the height of CG from the roll center. Note that the lateral force from gravity due to the road bank angle, ϕ_r, appears in Eq. (17), which describes the vehicle lateral dynamics, and the time derivative of p_f affects the vehicle roll dynamics in Eq. (19). The change of p_f, the roll rate of the vehicle frame, is related to the change of the road bank angle through Eq. (14) since the vehicle frame is assumed to keep contact on the ground.

From Eq. (17), (18), and (19), the following four-state linear model can be written in the state space form:

$$\dot{x} = Ax + B\delta + B_{w1}\phi_r + B_{w2}\dot{p}_f \qquad (20)$$

where

$$x = \begin{bmatrix} \beta & r_f & \phi_v & \dot{\phi}_v \end{bmatrix}^T$$

$$A = \begin{bmatrix} -\frac{I_{eq}C_0}{I_x m u_x} & -1 - \frac{I_{eq}C_1}{I_x m u_x^2} & \frac{h(mgh-k_r)}{I_x u_x} & -\frac{hb}{I_x u_x} \\ -\frac{C_1}{I_z} & -\frac{C_2}{I_z u_x} & 0 & 0 \\ 0 & 0 & 0 & 1 \\ -\frac{C_0 h}{I_x} & -\frac{C_1 h}{I_x u_x} & \frac{mgh-k_r}{I_x} & -\frac{b_r}{I_x} \end{bmatrix}$$

$$B = \begin{bmatrix} \frac{I_{eq}C_{\alpha f}}{I_x m u_x} & \frac{aC_{\alpha f}}{I_z} & 0 & \frac{C_{\alpha f}h}{I_x} \end{bmatrix}^T$$

$$B_{w1} = \begin{bmatrix} -\frac{g}{u_x} & 0 & 0 & 0 \end{bmatrix}^T$$

$$B_{w2} = \begin{bmatrix} 0 & 0 & 0 & -1 \end{bmatrix}^T$$

Note that the road bank angle, ϕ_r, and the time derivative of p_f are treated as disturbances or unknown inputs to the vehicle dynamics while the vehicle roll angle, ϕ_v, is a state resulting from the road bank angle and other inputs.

IV. Vehicle State Estimation

In order to implement a disturbance observer for estimating road bank angles, accurate measurements of the sideslip angle, β, are also necessary. While the yaw rate and roll rate of the vehicle can be easily measured using conventional rate gyros on the vehicle body, the sideslip angle cannot. Two common techniques for estimating this value are to integrate inertial sensors directly and to use a physical vehicle model. Some methods use a combination or switch between these two methods appropriately based on vehicle states [3], [9]. Direct integration methods can accumulate sensor errors and unwanted measurements from road grade and bank angle. In addition, methods based on a physical vehicle model can be sensitive to changes in the vehicle parameters and maneuvers outside in the linear region.

To overcome these drawbacks, a new method for estimating vehicle sideslip angle using GPS and INS sensor measurements has been presented by the authors [6]. In this scheme, GPS measurements from a two-antenna system are combined with INS sensor measurements to eliminate errors due to direct integration. Since both the vehicle

heading and the direction of velocity are directly measured from a two-antenna GPS receiver, the sideslip angle can be calculated as the difference between the two. INS sensors are integrated with GPS measurements to provide higher update rate estimates of the vehicle states and to handle periods of GPS signal loss. This method is also independent of any parameter uncertainties and changes because it is based on purely kinematic relationships. In addition to the sideslip angle, the sum of road bank and vehicle roll angles is similarly estimated in this scheme. Roll rate gyro measurements are integrated with the GPS roll measurements.

Fig. 3. Test Vehicle with Two-Antenna GPS Set-up

Fig. 3 shows the test vehicle used for experimental tests. Note that the sum of road bank and vehicle roll angle ($\phi_v + \phi_r$) can be directly measured by the two laterally placed GPS antennas.
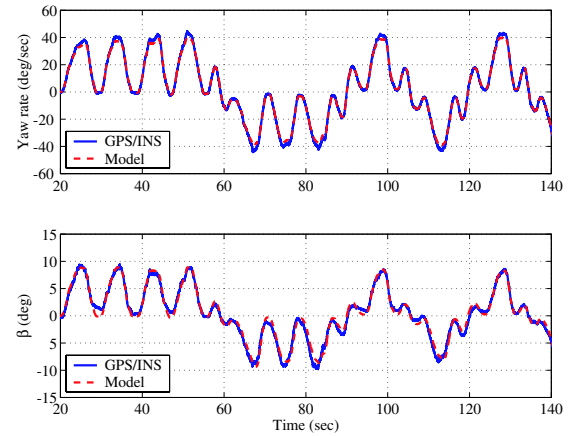

Fig. 4. Yaw Rate and Sideslip Angle Estimates

Experimental results from the GPS/INS integration are plotted in Fig. 4 on top of simulation results from the vehicle model for both yaw rate and sideslip angle. The estimates of the states match well with the simulation results. Further validation can be found in [10]. In fact, the estimated sideslip angle is accurate and clean enough to be

used for steer-by-wire control systems as a feedback signal [11]. The similarity between estimated and simulated yaw rates indicates that the vehicle model used in the comparison is valid and calibrated correctly.

Using this system, a disturbance observer can be implemented from the following available measurements:

$$y = \begin{bmatrix} \beta \\ r_m \\ \phi_v + \phi_r \\ p_m \end{bmatrix} = \begin{bmatrix} \beta \\ r_f \\ \phi_v + \phi_r \\ \dot{\phi}_v + p_f \end{bmatrix} \quad (21)$$

The yaw rate, r_f, and the sum of the vehicle roll rate and the rate of change of the roll angle of the vehicle frame, $\dot{\phi}_v + p_f$, are from the rate gyros according to Eq. (12) and (15). The sideslip angle, β, and the sum of the vehicle roll and road bank angle, $\phi_v + \phi_r$, are from the integration of GPS and INS.

V. DISTURBANCE OBSERVER

The road bank angle, ϕ_r, and the time derivative of p_r are the two disturbances to the vehicle dynamics described in Eq. (20). Since the road changes independently, the disturbances due to the road vary independently of the vehicle dynamics. However, the two disturbances are not independent of each other as shown in Eq. (14). Therefore, dynamics of the disturbances can be described as follows assuming that the disturbances due to the road changes are the result of white noise forcing $\ddot{p}_f$ and $\dot{\varepsilon}_r$ [5].

$$\dot{w} = A_w w \quad (22)$$

where

$$w = \begin{bmatrix} \phi_r \\ p_f \\ \dot{p}_f \\ \varepsilon_r \end{bmatrix}, \quad A_w = \begin{bmatrix} 0 & 1 & 0 & 1 \\ 0 & 0 & 1 & 0 \\ 0 & 0 & 0 & 0 \\ 0 & 0 & 0 & 0 \end{bmatrix}$$

From Eq. (20) and (22), a disturbance observer can be implemented by augmenting the disturbances to the state vector. A new state vector z is defined by augmenting w to the vehicle state vector x.

$$\dot{z} = \begin{bmatrix} A & B_w \\ 0 & A_w \end{bmatrix} z + \begin{bmatrix} B \\ 0 \end{bmatrix} \delta = Fz + G\delta \quad (23)$$

where

$$z = \begin{bmatrix} x & w \end{bmatrix}^T, \quad B_w = \begin{bmatrix} B_{w1} & 0 & B_{w2} & 0 \end{bmatrix}$$

The available measurements are from Eq. (21):

$$y = \begin{bmatrix} \beta \\ r_f \\ \phi_v + \phi_r \\ \dot{\phi}_v + p_f \end{bmatrix} = \begin{bmatrix} 1 & 0 & 0 & 0 & 0 & 0 & 0 & 0 \\ 0 & 1 & 0 & 0 & 0 & 0 & 0 & 0 \\ 0 & 0 & 1 & 0 & 1 & 0 & 0 & 0 \\ 0 & 0 & 0 & 1 & 0 & 1 & 0 & 0 \end{bmatrix} z \quad (24)$$

Since the new system from Eq. (23) and (24) is observable, a disturbance observer is given by the following equation:

$$\dot{\hat{z}} = F\hat{z} + Gu + L(y - H\hat{z}) \quad (25)$$

The corresponding error dynamics are then described as follows:

$$\dot{\tilde{z}} = (F - LH)\tilde{z} \quad (26)$$

where

$$\tilde{z} = z - \hat{z}$$

When the observer gain, L, is selected so that $F - LH$ has stable eigenvalues and the error dynamics are significantly faster than the system dynamics, or by applying a Kalman filter, the error dynamics approach zero [12]. In this paper, a Kalman filter is applied to determine the observer gain.

VI. EXPERIMENTAL RESULTS

A Mercedes E-class wagon is used for the experimental tests. The test vehicle is equipped with a 3-axis accelerometer/gyro triad and a two-antenna GPS system. The parameters of the vehicle model are accurately estimated using GPS measurements from a two-antenna system combined with INS sensors [6].

Fig. 5 shows experimental results for estimating vehicle roll and road bank angles using the proposed disturbance observer. Experimental tests consisting of four laps around an uneven surface are performed.
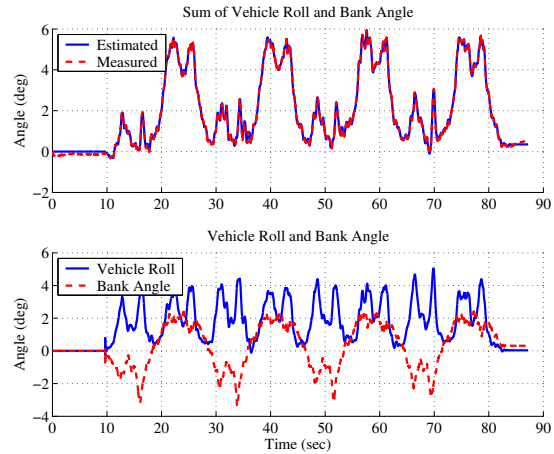

Fig. 5. Vehicle Roll and Bank Angle Estimates

The lower plot shows estimated vehicle roll and road bank angles individually, and the upper plot shows the sum of those two estimated values compared with the measured value using the two-antenna GPS setup combined with INS. Note that the sum of vehicle roll and road bank angles is mainly positive even though the road bank angle alone fluctuates almost evenly between positive and negative values. As easily seen in Fig. 5 at around 30, 50, and 70 seconds, a small value of the roll angle measurement – the sum of vehicle roll and road bank angles – does not necessarily mean a small vehicle roll angle and small road bank angle. A significant road bank angle can be a major factor in transient maneuvering, which is the cause of most rollover accidents.
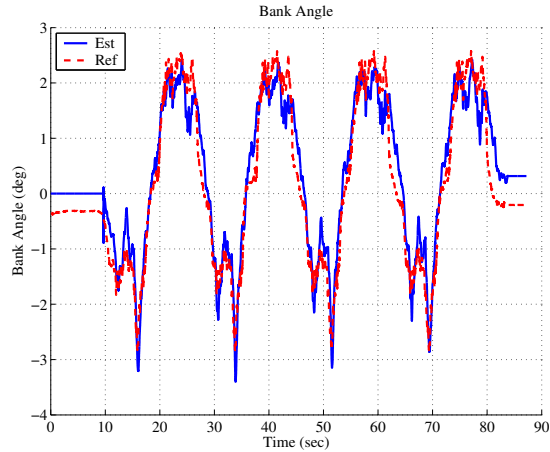
Fig. 6. Verification of Road Bank Angle Estimates

Fig. 7. Measured Lateral Acceleration and Estimates of Vehicle Roll and Bank Angles

To verify the estimates of the road bank angle, the true road bank angle is measured using a two-antenna GPS setup. The two GPS antennas are placed laterally on the top of the vehicle, and record the static roll angle as the vehicle moves along the marked path at a very low speed to avoid exciting vehicle roll dynamics. Since the measured roll angle from GPS contains both the road bank angle and the vehicle roll angle, the vehicle roll angle is then calculated from the estimated roll stiffness and subtracted from total roll angle [6]. The remaining angle is assumed to be the true road bank angle and is validated by repeating this test in the opposite direction of travel.

The estimated road bank angle from the proposed method is verified with this measured road bank angle in Fig. 6. The estimates match to within the accuracy of the static road bank measurement technique, suggesting that dynamic separation works well. In addition, slalom maneuvers on a fairly flat surface are performed to validate the estimation method. Fig. 7 shows estimated vehicle roll and road bank angles from the slalom maneuvers as well as measurements of the vehicle lateral acceleration.

As expected, the estimated road bank angle is very small (mostly less than one degree), which reflects the fact that the test is performed on a fairly flat surface. The estimated vehicle roll angle also shows strong correlation with the measured lateral acceleration, which can be predicted from the vehicle roll dynamics only when the effects from road bank are insignificant.

VII. Conclusion

A properly formulated disturbance observer and measurements from the GPS and INS sensors can separately estimate road bank angle and vehicle roll. These results can be used for a wide variety of applications including vehicle stability control systems, state estimators, and vehicle 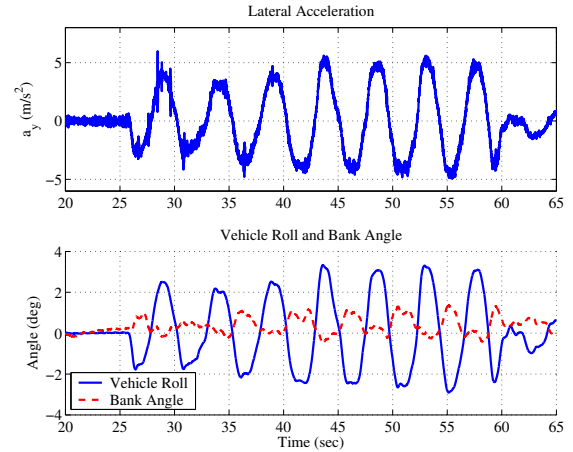rollover warning and avoidance systems. The possibility of estimating the vehicle roll and road bank angles without GPS measurements is currently under investigation.

VIII. Acknowledgements

The authors would like to thank the Robert Bosch Corporation for providing the test vehicle and sensors.

References

[1] H. E. Tseng *et al.*, "Development of vehicle stability control at ford," *IEEE/ASME Transactions on Mechatronics*, vol. 4, no. 3, pp. 223–234, 1999.

[2] A. Y. Ungoren, H. Peng, and H. E. Tseng, "Experimental verification of lateral speed estimation methods," in *Proceedings of AVEC 2002 6th Int. Symp. on Advanced Vehicle Control*, Hiroshima, Japan, 2002.

[3] A. Nishio *et al.*, "Development of vehicle stability control system based on vehicle sideslip angle estimation," 2001, sAE Paper No. 2001-01-0137.

[4] H. E. Tseng, "Dynamic estimation of road bank angle," *Vehicle System Dynamics*, vol. 36, no. 4-5, pp. 307–328, 2001.

[5] J. Hahn *et al.*, "Road bank angle estimation using disturbance observer," in *Proceedings of AVEC 2002 6th Int. Symp. on Advanced Vehicle Control*, Hiroshima, Japan, 2002.

[6] J. Ryu, E. Rossetter, and J. Gerdes, "Vehicle sideslip and roll parameter estimation using gps," in *Proceedings of AVEC 2002 6th Int. Symp. on Advanced Vehicle Control*, Hiroshima, Japan, 2002.

[7] R. Goldman, M. E. Gindy, and B. T. Kulakowski, "Rollover dynamics of road vehicles: Literature survey," *Heavy Vehicle Systems*, vol. 8, no. 2, pp. 103–141, 2001.

[8] C. R. Carlson and J. Gerdes, "Optimal rollover prevention with steer by wire and differential braking," in *Proceedings of IMECE 2003 ASME Int. Mechanical Engineering Congress and Exposition*, Washington, D.C., 2003.

[9] Y. Fukada, "Estimation of vehicle slip-angle with combination method of model observer and direct integration," in *Proceedings of AVEC 1998 4th Int. Symp. on Advanced Vehicle Control*, Nagoya, Japan, 1998.

[10] J. Ryu and J. Gerdes, "Integrating inertial sensors with gps for vehicle dynamics control," *ASME Journal of Dynamic Systems, Measurement, and Control*, To be appeared in June, 2004.

[11] P. Yih, J. Ryu, and J. Gerdes, "Modification of vehicle handling characteristics via steer-by-wire," in *Proceedings of the 2003 American Control Conference*, Denver, Co, 2003.

[12] A. Gelb *et al.*, *Applied Optimal Estimation*. Cambridge, Massachusetts: The M.I.T. Press, 1974.